

Accuracy Improvement of Counting Asbestos in Particles using a Noise Redacted Background Subtraction

Hikaru Kumagai, Soichiro Morishita, Kuniaki Kawabata, Hajime Asama and Taketoshi Mishima

Abstract—Increased health damage caused by asbestos has become a problem recently. Removal of asbestos contained in building materials and rendering it harmless is a common means of alleviating asbestos hazards, but that process necessitates a judgment of whether asbestos is included in building materials. According to an official method, particles and asbestos must be counted in a sample to judge whether it contains asbestos. This work is performed visually and requires enormous amounts of time and effort. Consequently, automated counting using background subtraction is proposed for rapid, highly accurate analysis. However, the method does not enable accurate counting because of noise included in a background image. This study is intended to improve the accuracy of counting particles through noise removal using a Gaussian filter.

I. INTRODUCTION

Health hazards such as malignant mesothelioma from exposure to asbestos have become a problem. As a measure against growing asbestos problems, asbestos analyses to check asbestos contents in building materials are performed widely. Dispersion staining is a qualitative analytical method to assess whether asbestos is contained in building materials. According to an official method [1] to assay three kinds of asbestos used commercially, it is necessary to make nine samples and count 3000 particles by microscopic observation from three samples that have been stained by immersion in liquid. Part of one such photomicrograph is presented in Fig. 1.



Fig. 1. Example of microscopic appearance of asbestos

Counting particles and asbestos is performed visually (Fig.

This work was supported by Ministry of the Environment Sciences Research Grants.

H. Kumagai and T. Mishima are with Department of Information and Computer Sciences Faculty of Engineering, Saitama University, 255 Shimo-Okubo, Sakura-ku, Saitama-shi, Saitama 338-8570, Japan (e-mail: {kuma,takemi}@me.ics.saitama-u.ac.jp)

S. Morishita and H. Asama are with Research into Artifacts, Center of Engineering, The University of Tokyo, 5-1-5 Kashiwanoha, Kashiwa-shi, Chiba 277-8568, Japan (e-mail: {mori,asama}@race.u-tokyo.ac.jp)

K. Kuniaki is with Intelligent System Research Unit, RIKEN, 2-1 Hirosawa, Wako-shi, Saitama 351-0198, Japan (e-mail: kuniakik@riken.jp)

2). It requires enormous amounts of time and effort. This process particularly makes asbestos analysis onerous and costly.



Fig. 2. Expert on counting particles and asbestos

There is a literature reported detecting cells in microscope images [2], but it is difficult for images containing variously shaped particles to use the method that depends on target shape. Noise removal and binarization are used for automated counting of pollen [3] and screening of *Bacillus thuringiensis* [4] to support analyses that are both rapid and highly accurate. Therefore, automated counting [5] using these approaches with background subtraction is proposed. However, the variance of some errors resulted from counting particles is large because of noise contained in a background image, the method does not enable accurate counting. The present study is intended to improve the accuracy of counting particles using image processing. We remove the noise using a Gaussian filter for a background image. Section II describes an automated counting method using background subtraction and a Gaussian filter.

II. THEORY

A. Automated Counting using Background Subtraction

1) identification of candidate regions of particle

We convert an original image and a background image (an image whose scanning condition is the same as the original image and is not contained in a sample) to a gray scale. Then we execute a labeling processing on some candidate regions of particles that were identified by taking subtraction of them. By taking subtraction of the original image and the background image, which have similar bias, we can almost entirely offset the bias. Fig. 3 shows that the bias has properties by which the pixel value in the center of the image is the largest; it ratchets down concentrically. There is a literature reported modeling of the illumination effects [6], but it

is difficult for each microscope image that has different bias to use the model.

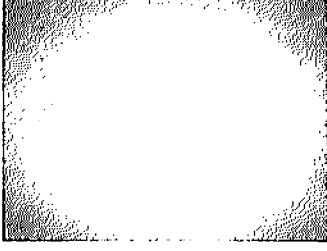


Fig. 3. Bias shown in the original image and the background image

We output the brightness of the original image to pixels whose difference is greater than 8, and output 0 to the pixel whose difference is less than 8.

2) detection of particles

We determine a threshold value of every detected candidate region of particles to divide particles of closely contacted regions; then we binarize them. Here, we use discriminant analysis method as a threshold value determination method. Discriminant analysis method classifies the histogram of brightness into two groups because of a threshold t , and determines threshold t whose ratio of interclass variance and intraclass variance is maximum. This method is represented as

$$\sigma_B^2(t) = \frac{\sum_{k=0}^{t-1} n_k (\bar{f}_0 - \bar{f})^2 + \sum_{k=t}^{255} n_k (\bar{f}_1 - \bar{f})^2}{\sum_{k=0}^{255} n_k} \quad (1)$$

$$\sigma_I^2(t) = \frac{\sum_{k=0}^{t-1} n_k (k - \bar{f}_0)^2 + \sum_{k=t}^{255} n_k (k - \bar{f}_1)^2}{\sum_{k=0}^{255} n_k}, \quad (2)$$

where σ_B^2 is the interclass variance, σ_I^2 is the intraclass variance, \bar{f}_0 is the average of pixel value that is in the range $0 \sim t-1$ when we binarized the gray scale image to a threshold t , \bar{f}_1 is the average of pixel value that is in the range $t \sim 255$, \bar{f} is the average of all pixel value in the image, and n_k is the number of pixels whose pixel value is k . Furthermore, we binarize the image using t as a threshold that maximizes the variance ratio, which is given as

$$F_0(t) = \frac{\sigma_B^2}{\sigma_I^2}. \quad (3)$$

We binarize all candidate regions using the threshold value determination method. There is certainly a particle in candidate regions of particles.

3) counting particles

We count particles that were detected using labeling processing. Specifically, we perform two-four-neighborhood labeling plus one-eight-neighborhood labeling using a raster scan.

Fig. 4 depicts a flowchart of the automated counting method and images that are output by it.

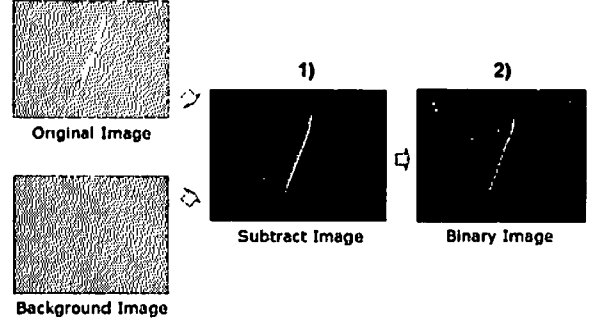


Fig. 4. Outline of conventional method

B. Brightness Normalization

The difference between maximum brightness and minimum brightness of an image for this study is small. Consequently, we normalize the brightness of the image and expand the dynamic range of the image signal. Therefore, if a brightness range exists whose occurrence frequency is 0 in the histogram of the image, subtle brightness changes can be made visible using the overall brightness range (Fig. 5). For example, brightness normalization is performed to remove the influence of the literal image because of heterogeneity for automated recognition and detection of signs in the natural scene [7].

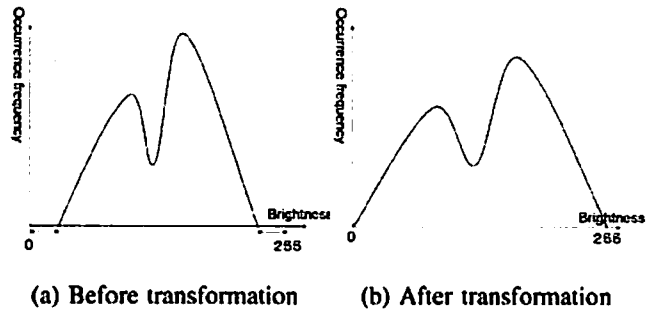


Fig. 5. Expansion of brightness dynamic range

In this work, we use linear transformation as a means for brightness transformation. Linear transformation transforms the input brightness x into output brightness y

$$y = ax + b. \quad (4)$$

Fig. 6 shows an example of linear transformation.

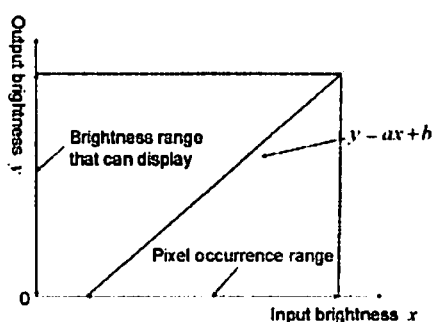
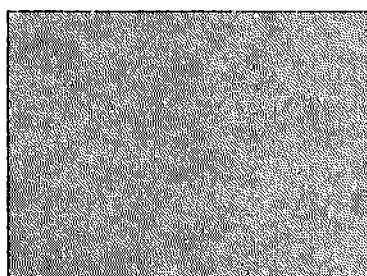
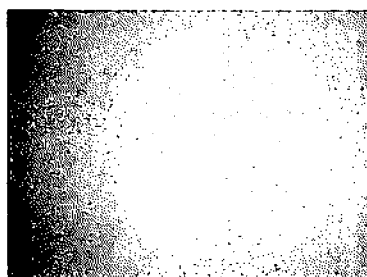


Fig. 6. Linear transformation

Fig. 7(a) shows an example of a background image. Fig. 7(b) shows an image that is normalized by Fig. 7(a).



(a) Before normalization



(b) After normalization

Fig. 7. Brightness normalization of a background image

Although Fig. 7(a) resembles a smooth image that has no particles, Fig. 7(b) is very rough because of noise. We think that this noise is bias by a light microscope with additional random noise from the CCD. Because of bias, the brightness changes smoothly from the inside of an image to the outside. Bias is offset using background subtraction. The regularity of bias must be preserved when noise is removed.

C. Fourier Transform

By analyzing frequency using two-dimensional Fourier transform, we evaluate the periodicity of brightness change depending on coordinates on the image. For example, some studies have analyzed spatial frequency components of noise [8]. A two-dimensional Fourier transform figure of the image $f(x,y)$ is presented as

$$F(u,v) = \mathcal{F}\{f(x,y)\} = \iint_{-\infty}^{\infty} f(x,y) \exp\{-2\pi j(ux + vy)\} dx dy. \quad (5)$$

Here, u, v is the spatial frequency. The properties held and sensations caused by the external surface of objects received through the tactile sense are called texture. These properties are obtained using a Fourier transform. The power spectrum $|F|^2$ is defined as (5), which presents the overall properties of the image.

Fig. 8 shows a power spectrum of Fig. 7(a). The frequency component that is in the center of the image is the low-frequency component: more spectrum information that is outside implies more high-frequency components.

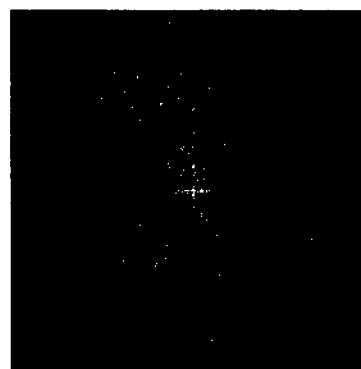


Fig. 8. Power spectrum of Fig. 7(a)

The frequency component in Fig. 8 is uniformly distributed. Fig. 7(a) shows a large high-frequency component.

D. Using a Gaussian Filter

A background image has high-frequency noise and a bias whose brightness changes smoothly from the inside of the image to the outside. We show it by normalizing brightness of images and analyzing frequencies using two-dimensional Fourier transform. This paper presents removal of noise using a Gaussian filter whose kernel size is determined arbitrarily for a background image and evaluating some errors that

resulted from counting particles by removing noise. A Gaussian filter is used for approximate acquisition of illumination information in the input image for information extraction that is robust against illumination changes [9]. A Gaussian filter in two dimensions smoothes an image according to a Gauss function that is given as

$$G(x,y) = \frac{1}{2\pi\sigma^2} \exp\left(-\frac{x^2+y^2}{2\sigma^2}\right), \quad (6)$$

where σ is given as

$$\sigma = \left(\frac{n}{2} - 1\right) \times 0.3 + 0.8 \quad (7)$$

in the Open Source Computer Vision Library (OpenCV), where n depends on the kernel size. Fig. 9 depicts part of a background image (a) without a Gaussian filter and (b) with it.



(a) Without a Gaussian filter (b) With a Gaussian filter

Fig. 9. Part of a gray-scale background image

We can confirm conservation of bias and removal of high-frequency noise. Furthermore, 10 shows a power spectrum of Fig. 7(a) for which we used a Gaussian filter whose kernel size is 3×3 . We compare Fig. 8 to Fig. 10. The frequency component in Fig. 10 is concentrated in the center. Therefore, the high-frequency component in background image Fig. 7(a) is removed using a Gaussian filter.



Fig. 10. Power spectrum of Fig. 7(a) with a Gaussian filter

Methods of noise removal such as Median filter [10], dilation and erosion [11] are also used for image processing. Although they are available for binary images, we do not use them to remove noise from a target image in this study.

III. EXPERIMENT

A. Steps

- 1) We use a Gaussian filter for a background image, and count particles according to section II-A.
- 2) We consider false positives and false negatives. Then we evaluate the differences between the counted particles and actual particles.
- 3) We show a distribution of counting errors using a boxplot.
- 4) We evaluate averages p of the counted particle rate, false positive rate, and false negative rate, which is given as

$$p = 100.0 \times \frac{1}{N} \sum_{i=1}^N \frac{n_i}{v_i}, \quad (8)$$

where N is the number of samples, n_i is the number of counting particles or false positives or false negatives for the i -th image and v_i is the number of actual particles for the i -th image.

Regarding an evaluation of counting particle rate, classification of sample images is presented in Fig. 11 because the number of particles differs among images.

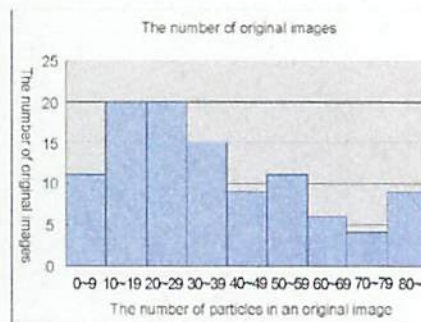


Fig. 11. Histogram of sample images

We judge true or false counting by comparing an output image with the image that is counted by an expert. An example of an image that has been counted by an expert is presented in Fig. 12.

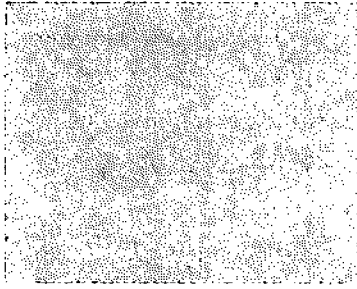


Fig. 12. An image for which particles were counted by an expert

B. Results

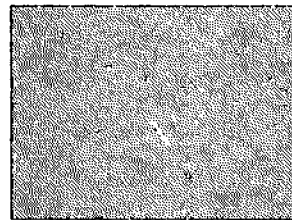
Fig. 13(c) shows an output image of automated counting using a background image without a Gaussian filter. Fig. 13(d) shows an output image of obtained by automated counting using a background image with a Gaussian filter whose kernel size is 7×7 . The number of actual particles is 74, but particles that were counted using conventional method (using a background image without a Gaussian filter) were 95 because of the influence of noise, which is seen in red and yellow circles. Then the particles counted using the proposed method (using a background image with a Gaussian filter) are 88 because of noise reduction that is seen in these circles; the number of counted particles approaches the number of actual particles.

Fig. 14(a) shows a boxplot that presents the distribution of counting errors for the result obtained using background subtraction using a background image without a Gaussian filter. Fig. 14(b) shows a boxplot that presents results obtained using a background image with a Gaussian filter. The distribution of counting errors in Fig. 14(a) is wide overall. Nevertheless the distribution in Fig. 14(b) approached 0 overall, indicating that the variance of the proposed method is less than that of the conventional method.

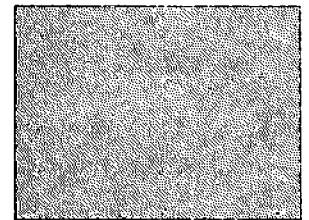
Table I presents the number of counted particles, false positives, false negatives, and the average counted particles rate, false positive rates, and false negative rates denoted as in Eq. (8)

It is good that the counted particles are approximately equal to the number of actual particles: 3930 in 105 original images. The number of false positives and false negatives are almost 0, and the averages of each counting rate are near 100%. Furthermore, a sample containing asbestos can be judged as a harmless sample because of false positives, we particularly emphasize that false positive data decreased.

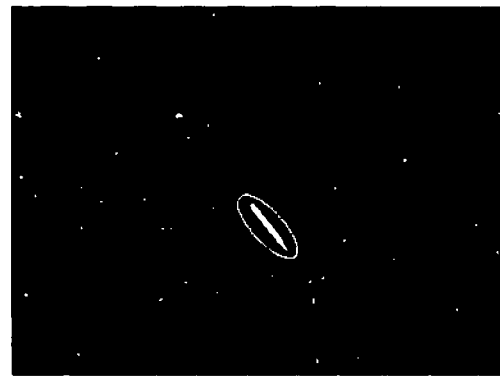
However, the false positive rate of 33.4% is not sufficient, and it must be improved more.



(a) Original image



(b) Background image

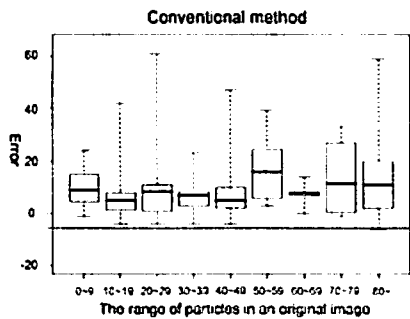


(c) An output image obtained using the conventional method

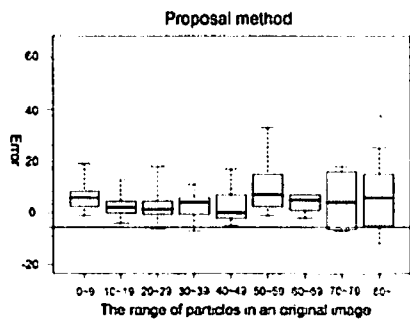


(d) An output image obtained using the proposed method

Fig. 13. An example of output images



(a) A boxplot of results obtained using the conventional method



(b) A boxplot of results obtained using the proposed method

Fig. 14. Distribution of counting errors

TABLE I
EXPERIMENT RESULTS

Result \ Approach	Conventional	Proposed
Counted particles	4960	4372
Counted particle rate (%)	143.8	120.8
False Positive	1471	887
False Positive rate (%)	56.3	33.4
False Negative	441	431
Average of False Negative rate (%)	12.5	12.5

IV. CONCLUSIONS AND FUTURE WORK

This study is intended to improve the accuracy of automated counting of particles. For removal of noise included in a background image, we used a Gaussian filter. Results demonstrate that the accuracy of counting particles was improved by noise removal. Future works shall determine the proper parameters of the Gauss function and elucidate differences in the characteristics of noise and particles.

REFERENCES

- [1] H. Shima, "JIS A 1481 Determination of asbestos in building material products", Japanese Standards Association, 2006.
- [2] T. W. Natkemper, H. Wersing, W. Schubert, and H. Ritter, "A neural network architecture for automatic segmentation of fluorescence micrographs", In *Proc. European Symp. Artificial Neural Networks*, pp. 177-182, 2000.
- [3] S. Kawashima, Y. Takahashi, S. Aikawa, and T. Nagoya, "An Attempt of Applying the Image Processing for the Automatic Estimation of Sampled Airborne Pollen", *Japanese Journal of Allergology*, vol. 44, no. 9, pp. 1150-1158, 1995.
- [4] T. Hyakutake, T. Ichimatsu, E. Mizuki, and M. Ohba, "A Rapid Screening Technique for *Bacillus thuringiensis* Using Image Processing", *Japanese Journal of Applied Entomology and Zoology*, vol. 45, no. 1, pp. 9-14, 2001.
- [5] Y. Komori, "Development of Method for Analyzing Asbestos Using Image Processing", Bachelor Thesis, 2006.
- [6] T. Whitted, "An Improved Illumination Model for Shaded Display", *Communications of the ACM*, vol. 23, no. 6, pp. 343-349, 1980.
- [7] X. Chen, J. Yang, J. Zhang, and A. Waibel, "Automatic detection and recognition of signs from natural scenes", *IEEE Transactions on Image Processing*, vol. 13, no.1, pp. 87-99, 2004.
- [8] S. Yamada and K. Murase, "Analysis of the Frequency Components of CR Portal Images and Application to Multi-objective Frequency Processing", *Japanese Journal of Radiological Technology*, vol. 59, no. 7, pp. 864-871, 2003.
- [9] H. Wang, S. Z. Li and Y. Wang, "Face recognition under varying lighting conditions using self-quotient image", *Proc. of the Sixth IEEE International Conference on Automatic Face and Gesture Recognition*, 2004, pp. 819-824, 2004.
- [10] J.W. Tukey, "Nonlinear (nonsuperimposable) methods for smoothing data", *Cong. Rec. EASCON*, pp. 673, 1974.
- [11] M. Bomans, K. H. Hohne, U. Tiede and M. Riemer, "3-D segmentation of MR images of the head for 3-D display", *IEEE Transactions on Medical Imaging*, vol.9, 177-183, 1990.